STRUCTURATION INVESTIGATION OF FAST - SETTING SELF LEVELING UNDERLAYMENT BASED ON ETTRINGITE BINDER

N.N. LAM[1]

Self – Levelling Underlayment (SLU) is one of the high-performance new materials used in the construction industry. Besides the strength, other characteristics of SLU such as workability, rapid drying, rapid hardening, shrinkage compensation, smooth nature, etc. are required depending on the application. The aim of this study is to evaluate the structuration with the time of SLU through some important characteristics such as the evolution of rheological properties, ettringite, and gibbsite phase development. To this purpose, a rheometer with rotation mode and oscillation mode was used to determine the yield stress, plastic viscosity, rheological dynamic modulus (storage modulus and loss modulus). The use of these techniques is considered to be a method for monitoring structuration development in cement materials. The result shows that during the hydration process, increased plastic viscosity, yield stress, and dynamic modulus of the SLU were identified from just 5 minutes after mixing until the setting period when the transition from a fluid state to a solid-state of SLU takes place. By using a rheometer in oscillation mode, the beginning of the transition process from the liquid-state to the solid-state of SLU was identified, this method is more precise when compared to traditional Vicat method.

Keywords: Structuration, Self – levelling underlayment, Fast-setting, Ettringite.

---

[1] PhD., Hanoi University of Civil Engineering, Faculty of Building Materials, 55 Giai Phong Road, Hai Ba Trung District, Hanoi, Viet Nam, e-mail: lamnn@nuce.edu.vn

1. INTRODUCTION

Due to the high flowability and self-smoothing properties, self-leveling underlayment (SLU) has been studied in recent years for concrete floors in various fields such as office buildings, apartments, shops, schools, hospitals, factories, parking lots, vessels, and repairing works [1], [2], [3]. Along with the strength, other characteristics of SLU such as shrinkage compensation, rapid hardening, rapid drying, smooth nature, etc. are required. One of the innovative binders for SLUs is the ettringite binder [4], [5]. This binder includes calcium aluminate cement (CAC), different sources of calcium sulfate $(C\$H_x)$, and Portland cement (PC). The combination of this binder with special additives produces rapid setting and hardening, autodesiccation, and desiccation compensation for shrinkage [5], [6], [7], [8]. Hydration of an ettringite binder containing aluminum cement (CAC) and calcium sulfate $(C\$H_x)$ induces ettringite $(C_6A\$_3H_{32})$ and aluminum hydroxide (AH_3). The ettringite-based compound exhibits advantages compared to ordinary Portland cement because of their high early-age strength, good chemical resistance, and their ability to stabilize heavy metals within their structure [9], [10], [11]. Therefore, in order to achieve environmental and economic benefits while achieving high mechanical performance, the ettringite based binder can potentially partially replace the OPC. However, the number of researches on ettringite based binder is very limited, particularly on the characteristics at an early age of SLUs.

It is difficult to clearly define the term "early - age" in research binder, this period can be associated with the rapid hydration process after the contact between the binder with water, and leads to the development of the microstructure, the consequences of which are the structuring and change of macroscopic properties [12], [13] and the material passes from the liquid state to the solid-state. This phenomenon leads to the setting and increasing mechanical resistance.

The beginning of the structuration of ettringite based binder can begin at an early age, within a few minutes to a few hours and s' accompanied by a strong release of heat [14]. In general, it is considered that in the case of ettringite binders, the structuration ends 24 hours after mixing. But that depends on the mineral (or chemical) composition of the binder, the water/binder ratio, the temperature, and the nature of the additive [15]. In the field of cement chemistry, the setting time is one of the fundamental mechanical characteristics at a very early age because it conditions the implementation processes (mixing, transport, pumping, shaping, etc.). In the cement standard, the setting time indicator is provided by using the Vicat needle test. The simplicity of this test is its main advantage but also leads to an overly macroscopic indicator of the state of the structuring of the mixtures [16], [17]. In this study, the structuration process is studied from the monitoring of the evolution of the physical

parameters more related to the hydration of the material such as the yield stress, plastic viscosity, rheological dynamic modulus (storage modulus G' and loss modulus G") of SLUs.

2. MATERIALS AND METHODS

2.1. MATERIALS

Calcium aluminate cement (CAC), Portland cement CEM I (PC), and hemihydrate (P) are the main components used in binders of the fast-setting SLU. Table 1 demonstrates the chemical composition by X-ray fluorescence (XRF) analysis of these raw materials. The mineralogical compositions of the calcium aluminate cement and Portland cement in Table 2 were determined by X-ray diffraction (XRD) using Cu-Kα radiation. The skeleton of SLU composes of silica sand, slag, and limestone fillers with average diameters of 88.19 µm, 11.95 µm, and 1.38 - 24.96 µm, respectively.

Table 1. Chemical composition of different binders.

Raw materials	Principal oxides, wt%										
	Al_2O_3	CaO	SiO_2	Fe_2O_3	MgO	TiO_2	K_2O	Na_2O	SO_3	MnO	L.O.I
CAC	69.68	29.78	0.26	0.16	0.15	0.04	-	0.23	0.27	0.01	-
CEM I – 42.5	5.30	67.28	20.22	0.20	1.02	0.18	0.26	0.20	2.63	0.06	-
α-Hemihydrate	-	38.70	0.27	0.03	0.1	0.003	-	-	52.40	-	8.4

Table 2. Mineralogical compositions of CAC and PC.

Cement type	Percentage of phases, by weight %				
CAC	CA	CA_2	$C_{12}A_7$	C_2AS	$C_4A_3\$$
	57.70	37.50	0.35	0.65	1.07
CEM	C_3S	C_2S	C_3A	C_4AF	SO_3
	71.5	14.05	11.6	-	2.4

The formulation of fast- setting SLU based on ettringite binder is presented in Table 3:

Table 3. Formulation of fast- setting SLU.

Raw materials		Content, %
BINDER + SKELETON	CAC	24.26
	Hemihydrate	8.09
	PC	3.97
	Silica Limestone filler Slag	33.41
ADMIXTURES	Superplasticizer Viscosity Modifying Admixture Shrinkage reducing admixture	5.46
	Retarder Accelerator	0.238
Water		24.57
Total (%)		100

2.2. METHODS

2.2.1. VICAT NEEDLE PENETRATION

The Vicat needle test method is to determine the time of setting of hydraulic cement according to standard BS EN 196-3. However, in this study, to characterize the structuration with time of SLUs, this method was used by investigation of the penetration of Vicat needle.

2.2.2. INFRARED SPECTROSCOPY

Infrared spectroscopy (IR) technique is based on the absorption phenomenon that occurs when infrared radiation passes through a material. This method can be used to study crystalline and amorphous samples [18]. In this work, this technique makes it possible to identify the hydration products poorly crystallized or in small quantities. In order to study the structuration of fresh SLUs at the beginning, a Thermo Fisher Scientific IS50 device was used to realize infrared spectroscopy measurements.

The spectra are continuously recorded every minute for 24 hours. Acquisitions are made between 450 and 4000 cm^{-1}, the number of scans is 32 and the resolution is 4cm^{-1}. The investigation during the hydration of binder in SLUs can identify chemical bonds such as sulfate bonds associated with

ettringite or and with the formation of AH_3 thanks to the variations in the absorbance of the bands at 1100 cm^{-1} and 1020 cm^{-1} [19].

2.2.3. RHEOLOGICAL PARAMETERS

A parallel plate rheometer (MCR 301 Anton Paar plane-plane rheometer) was used to determine the rheological parameters of SLUs.

To measure the rheological properties of the materials the rheometer was equipped with serrated test plates (35 mm diameter). A gap between the two plates must be greater than the size of a particle in cement paste or mortar (normally the chosen gap is 10 times greater than the maximum particle size) [17]. Therefore, the gap between the plates has been fixed at 1.5 mm. A plastic box was used to enclose the specimen to limit water evaporation from the sample. Rheological properties can be determined in rotation mode or oscillatory mode.

2.2.3.1. ROTATION MODE

The rheometer enables the measurement of rheological parameters, namely yield stress and plastic viscosity by applying different deformation rates to SLUs in the rotation method. Fresh mortar or cement paste can be considered as a fluid material where the yield stress is the initial flow resistance caused by contact between particles, whereas the viscosity of the plastic controls the behavior once the torque required to initiate the motion has been achieved [20], [21]. The Bingham model could present the rheological behavior of cement-paste, mortars as follows:

$$\tau = \tau_0 + \mu_p \cdot \dot{\gamma} \qquad (1)$$

where τ (Pa) is the shear stress,

τ_0 (Pa) is the yield stress,

μ_p (Pa.s) is the plastic viscosity,

and $\dot{\gamma}$ (s^{-1}) is the shear rate.

The yield point of a material described in Figure 1 is the point at which the material will start to flow caused by that the external forces acting on the material are larger than the internal structural forces. The transition from elastic behavior to viscous behavior of materials gives information about its structuration versus times.
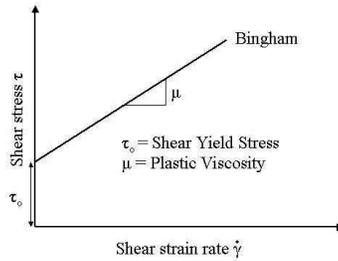
Figure 1. Bingham model [16].

In this study, to obtain the flow curve, the fresh SLUs were sheared by an increasing gradient from $0.1\ s^{-1}$ to $50\ s^{-1}$ with a step of $10\ s^{-1}$. The rheometer records shear strain as a function of shear rate, then the Bingham model calculated the plastic viscosity and yield stress.

2.2.3.2. OSCILLATION MODE

The principle of the dynamic mode is rheometer will apply a sinusoidal deformation with frequency ω to the material [22]:

$$\gamma(t) = \gamma_o.\cos(\omega t) \qquad (2)$$

In the case where the applied strain belongs to the linear viscoelastic region, the resulting shear stress is also sinusoidal and out of phase by a time δ with respect to deformation:

$$\tau(t) = \tau_0.\cos(\omega t + \delta) \qquad (3)$$

where: γ_0 and τ_0 are the shear strain and shear stress amplitude of oscillation respectively.

These modulus can also be used to describe the complex modulus, G^*, by the relation:

$$G^* = \tau_o/\gamma_o \qquad (4)$$

Recall that the oscillating stress of a viscoelastic material is in phase opposite with the phase of strain. The conservation modulus or storage modulus (G') and loss modulus (G") then can be written:

$$G' = G^*\cos\delta \qquad (5)$$

$$G'' = G^*\sin\delta \qquad (6)$$

Dynamic mode rheology has also been used to study the mechanical properties of cement pastes from mixing until setting [23], [24], [25]. In this study, to observe the structuring that takes place during the first minutes, the frequency of 1Hz and the deformation of 0.01% which is similar to that of Portland cement were selected to follow the structuration of SLUs [26].

3. RESULTS AND DISCUSSION

3.1. VICAT NEEDLE PENETRATION MEASUREMENT

By determining the Vicat needle penetration as continuously as possible, the structuration of SLUs with is thus characterized. The curve in Figure 2 shows the monitoring of Penetration of the Vicat needle as a function of time of the ettringite based SLU:
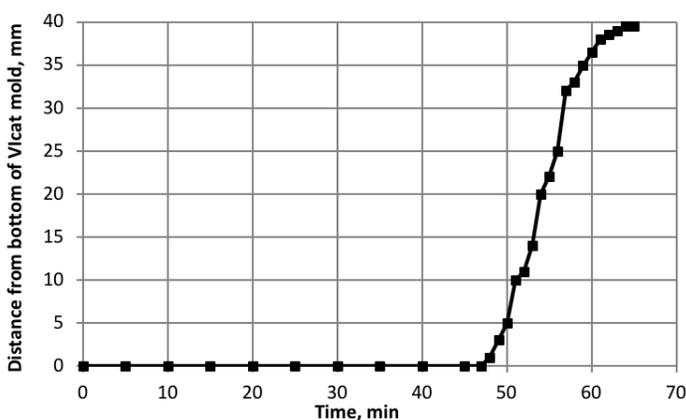

Figure 2. Penetration of the Vicat needle as a function of time.

The setting time of SLU is short, which means that the hydration and structuration of the fast-setting SLUs occur quickly after 50 minutes from contact of binders and water. After just over 15 minutes, the setting and solidification of SLU took place very strongly, this has practical implications in the construction of this material.

3.2. INVESTIGATION OF ETTRINGITE AND GIBBSITE SIGNAL BY IR TECHNIQUE

The infrared technique allows us to identify poorly crystallized products such as aluminum hydroxide (AH$_3$), ettringite, which are the main phases in ettringite binder. This technique has several advantages for monitoring the hydration of cement matrices based on the characteristics of this technique: speed, simplicity, continuity. As already discussed above, the evolution of the IR intensity of ettringite at the band 1100 cm^{-1} (Figure 3.a) and of AH$_3$ (Figure 3.b) at band 1020 cm^{-1} was realized up to 1000 minutes after mixing.
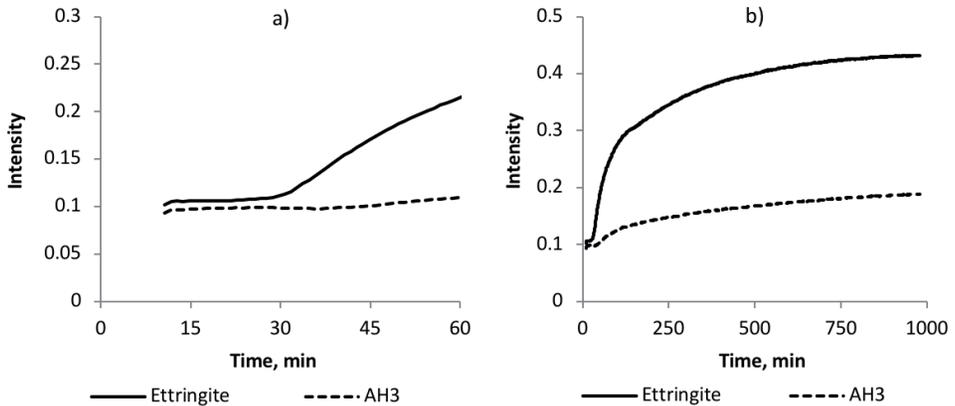
Figure 3. Augmentation of IR intensity versus time of SLU.

a) Until 60 mins after mixing.   b) Until 1000 mins after mixing.

The results in Figure 3 show that, in the first 30 minutes, the formation rate of ettringite and AH$_3$ occurred quite slowly, but after 30 minutes, the rate of formation of ettringite and AH$_3$ occurred quite strongly and gradually increased over time. This could be predicted that structuration of the mortars occur quickly 30 minutes after mixing with water. This result shows that the ettringite formation process took place faster than the moment of initial setting time of SLU according to the vicat needle penetration method. It can be explained by the fact that content of hydration product, especially ettringite is not large enough to lead to the solification and phase transition from liquid to solid of SLU.

3.3. RHEOLOGICAL PARAMETERS OF SLUs

3.3.1. RHEOLOGICAL PROPERTIES IN ROTATONAL MODE

The results versus time of yield stress and plastic viscosity of SLU is shown in Table 4 and Figure 4 As mentioned above, SLU can be considered as a fluid material, the Bingham model can describe rheological behavior of SLU as equation (1):

Table 4. Yield stress and plastic viscosity of SLU versus time.

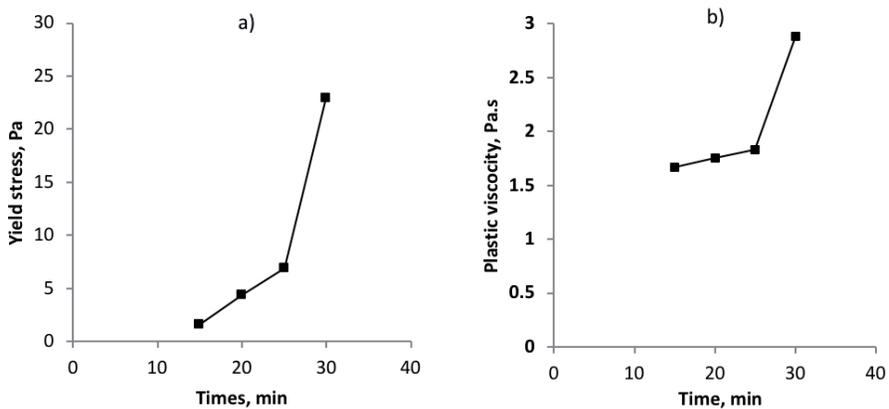| Time after mixing (minute)	Yield stress, τ_0 (Pa)	Plastic viscosity, μ_p (Pa.s)	R^2
15	1.58	1.66	0.963
20	4.38	1.75	0.976
25	6.93	1.83	0.968
30	22.95	2.88	0.882

Figure 4. Augmentation of yield stress and plastic viscosity versus time of SLU.

a) Yield stress.   b) Plastic viscosity.

The results in Figure 4 indicate that the yield stress and plastic viscosity increase slightly from 15 to 25 minutes after mixing. However, a rapid increase in yield stress and plastic viscosity from 25 to 30 minutes indicate sudden changes in SLU structuration increasing inter-granular friction and strengthen the cohesion in the SLU maxtrix. After 30 minutes, these SLUs start the transition from the liquid state to the solid-state and a setting period take places, the rheometer cannot apply shear rate as desired. Thus, the determination of viscosity and yield stress was stopped after 30 minutes from mixing the SLU with water. This result is similar and logical to the result obtained with Vicat needle and infrared spectroscopy measurement.

3.3.2. STRUCTURATION INVESTIGATON IN DYNAMIC MODE

With oscilation mode, the storage modulus G' and loss modulus G'' of SLU were followed by imposing a shear strain of 0.01% at a constant frequency f = 1Hz. The results relating to kinetics of these rheological modulus are shown in Figure 5:
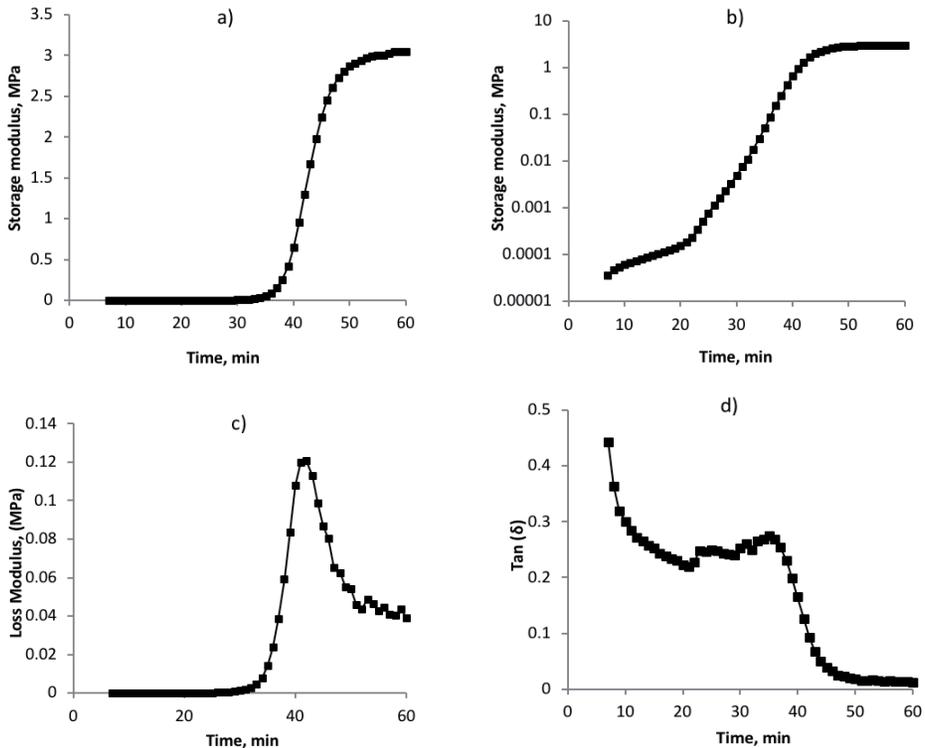

Figure 5. Evolution of rheological modulus versus time.

a) Storage modulus G' on a linear scale.   b) Storage modulus G' on a log scale.

c) Loss modulus G".   d) Tan (δ)=G''/G'.

These results are compatible with the results of rheology measurements (plastic viscosity and yield stress) mentioned above. The results in Figure 5.a and Figure 5.b show that the evolution of storage modulus G', which describes the SLUs structuration, in oscillatory mode is similar to that of yield stress and plastic viscosity in rotation mode before 30 minutes of mixing. Afterward, the storage modulus G' begins to increase rapidly after 30 minutes of mixing, then no longer increases with time (G' is about 3 MPa). While the loss modulus G'' in Figure 5.c from the beginning increases to a critical value, then it starts to go down. The peak of the loss modulus G'' indicates the maximum

consumption energy, and therefore, the maximum of the lost deformation energy. In Figure 5.d, the peak of the curve $\tan(\delta) = G''/G'$ indicates the maximum ratio G''/G' and therefore the maximum value of lost energy and storage energy in the deformation. It is found that the peak of $\tan(\delta)$ occurs at the moment where appears a sharp augmentation in the evolution of the loss modulus G'' and the storage modulus G' in about 30 minutes. Therefore, we can consider this peak $\tan(\delta)$ as the initial signal related to the structuration. Before 20 minutes, the SLU remains in the liquid state. The cohesion between the particles is not important, the energy dissipated due to friction between particles is always low. Therefore, the plastic viscosity and yield stress of SLU increase quite slowly during the first 20 minutes. However, when the degree of hydration increases, the hydrates were formed the more and more as a function of time and strengthened the cohesion in the mixture of the self-leveling compound, thus the viscosity of the matrix increases and results in lost energy which becomes more and more important and reaches a maximum. Then this peak $\tan(\delta)$ starts to decline after 30 minutes when the SLU becomes more elastic due to an increasing number of solid phases. Therefore, the $\tan(\delta)$ can be considers as the signal indicating the transition from the liquid state to the solid-state of SLU.

4. CONCLUSION

The evolution of the rheological properties at an early age of self – leveling underlayment until setting by detecting continually the changes in the structuration was studied, some conclusions can be withdrawn as follows:

- Hydration kinetics of ettringite and AH_3 formation over time has been determined. After 30 minutes from the time of mixing cement and water, the rate of hydration products formation took place quite strongly, especially ettringite, which determines the properties of SLUs at an early age. After 10 hours, the ettringite and AH_3 formation process begins to slow down.
- By using the rheometer in rotation mode, the transition from a liquid state to the solid-state of SLU was determined after 30 minutes of mixing. At this moment a rapid increase of yield stress and plastic viscosity, which realates to the structuration of SLU, take place.
- This result is suitable for the result achieved by oscillation mode. The peak of $\tan(\delta)$ after mixing 30 minutes begins to decrease, this moment corresponds to an increasing number of solid phases and a simultaneous increase in the storage modulus G' and the loss modulus G'' which reflects the hardening of the SLU.

- The beginning of the transition process from the liquid-state to the solid-state of SLU can be discovered by determination of Tan(δ). This parameter is more precise than the traditional Vicat Needle penetration method.

REFERENCES

1. M. Wallace, "Self-leveling underlayments - an easy way to level floors," Concr. Constr. - World Concr., vol. 32, no. 3, 1987.
2. Y. Guan, X. Zhou, X. Yao, and Y. Shi, "Vibration of cold-formed steel floors with a steel form deck and gypsum-based self-leveling underlayment," Adv. Struct. Eng., vol. 22, no. 13, pp. 2741–2754, 2019.
3. J. Kighelman, "Hydration and structure development of ternary binder system as used in self-levelling compounds," EPFL, Lausanne, 2007.
4. K. Onishi and T. A. Bier, "Investigation into relations among technological properties, hydration kinetics and early age hydration of self-leveling underlayments," Cem. Concr. Res., vol. 40, no. 7, pp. 1034–1040, 2010.
5. J. A. Elodie Prud'homme, Ngoc Lam Nguyen, Marie Michel, Jean-François Georgin, "Investigation of Ettringite Binder Hydration at Early Age for Glass Fiber Reinforced Concrete Application," in Developments in Strategic Materials and Computational Design V: A Collection of Papers Presented at the 38th International Conference on Advanced Ceramics and Composites, 2014.
6. E. Prud, T. Guillot, J. Ambroise, P. A. Andreani, and P. Taquet, "Critical analysis of residual water in self-leveling underlayment," Constr. Build. Mater., vol. 200, pp. 55–63, 2019.
7. H. Lutz and R. Bayer, "Dry Mortars," in Ullmann's Encyclopedia of Industrial Chemistry, 2010.
8. N. L. Nguyen, "Comparison of autogenous shrinkage measurements by different methods in case of fast-hardening mortar," in IOP Conference Series: Materials Science and Engineering, vol. 869, issue 3, pp. 032-041, 2020.
9. G. Le Saoût, B. Lothenbach, P. Taquet, H. Fryda, and F. Winnefeld, "Hydration of calcium aluminate cement blended with anhydrite," Adv. Cem. Res., vol. 30, no. 1, pp. 24–36, 2018.
10. S. Lamberet, "Durability of ternary binders based on portland cement calcium aluminate cement and calcium sulfate," École Polytechnique Fédérale de Lausanne, 2005.
11. N. N. Lam, "Some microstructure properties at early age of ettringite binder based on rich C12A7 calcium aluminate cement," J. Sci. Technol. Civ. Eng. - NUCE, vol. 12, no. 3, pp. 44–50, 2018.
12. L. Barcelo, M. Moranville, and B. Clavaud, "Autogenous shrinkage of concrete: A balance between autogenous swelling and self-desiccation," Cem. Concr. Res., vol. 35, no. 1, pp. 177–183, 2005.
13. E. E. Holt, "Early age autogenous shrinkage of concrete," VTT Publ., 2001.
14. J. F. Georgin and E. Prud'Homme, "Hydration modelling of an ettringite-based binder," Cem. Concr. Res., vol. 76, pp. 51–61, Oct. 2015.
15. Ngoc Lam Nguyen, "Influence of type of calcium sulfate on chemical shrinkage and heat of hydration in self-leveling underlayments using ettringite binder," J. Sci. Technol. Civ. Eng. - NUCE, vol. 12, issue.2, no. 2, pp. 92–97, 2018.
16. R. Ylmén, U. Jäglid, B. M. Steenari, and I. Panas, "Early hydration and setting of Portland cement monitored by IR, SEM and Vicat techniques," Cem. Concr. Res., vol. 39, no. 5, pp. 433–439, 2009.
17. T. G. Mezger, The Rheology Handbook. 2019.
18. A. Dutta, "Fourier Transform Infrared Spectroscopy," in Spectroscopic Methods for Nanomaterials Characterization, 2017, pp. 73–93.
19. R. B. Perkins, "The solubility and thermodynamic properties of ettringite, its chromium analogs, and calcium aluminum monochromate (3CaO*Al(2)O(3)*CaCrO(4)*nH(2)O))," 2000.
20. Rheology of Fresh Cement and Concrete. 1991.
21. M. Stieger, "The Rheology Handbook - For users of rotational and oscillatory rheometers," Appl. Rheol., 2019.
22. and W. G. L. L. J. Struble, H. Zhang, G.K. Sun, "Oscillatory shear behavior of Portland cement paste during early hydration," Concr. Sci. Eng. RILEM Publ. SARL, vol. 2, no. 7, pp. 141–149, 2000.
23. P. S. Nicoleau L., Garrault S., Nonat A., "Etude par rhéométrie dynamique des interactions physico-chimiques entre les latex et les phases minérales constituant le ciment," in 38ème colloque français du Groupe Français de Rhéologie., 2003.

24. L. Nachbaur, J. C. Mutin, A. Nonat, and L. Choplin, "Dynamic mode rheology of cement and tricalcium silicate pastes from mixing to setting," Cem. Concr. Res., 2001.
25. S. Gauffinet-Garrault, "The rheology of cement during setting," in Understanding the Rheology of Concrete, 2012, pp. 96–113.
26. S.H. Jang, "Identification of concrete incompatibilities using cement paste rheology," 2009.

LIST OF FIGURES AND TABLES: